

# DATA FUSION TOOL FOR SPIRAL BEVEL GEAR CONDITION INDICATOR DATA

Paula J. Dempsey  
National Aeronautics and Space Administration  
Glenn Research Center  
21000 Brook Park Rd.  
Cleveland, Ohio 44135  
Telephone: (216) 433-3398  
[Paula.J.Dempsey@nasa.gov](mailto:Paula.J.Dempsey@nasa.gov)

Lance J. Antolick, Jeremy S. Branning, and Josiah Thomas  
RMCI Inc.  
1525 Perimeter Parkway  
Huntsville, Alabama 35806

**Abstract:** Tests were performed on two spiral bevel gear sets in the NASA Glenn Spiral Bevel Gear Fatigue Test Rig to simulate the fielded failures of spiral bevel gears installed in a helicopter. Gear sets were tested until damage initiated and progressed on two or more gear or pinion teeth. During testing, gear health monitoring data was collected with two different health monitoring systems. Operational parameters were measured with a third data acquisition system. Tooth damage progression was documented with photographs taken at inspection intervals throughout the test. A software tool was developed for fusing the operational data and the vibration based gear condition indicator (CI) data collected from the two health monitoring systems. Results of this study illustrate the benefits of combining the data from all three systems to indicate progression of damage for spiral bevel gears. The tool also enabled evaluation of the effectiveness of each CI with respect to operational conditions and fault mode.

**Keywords:** Data fusion; diagnostics; gears; health monitoring

**Background:** Helicopter transmission health is important to aircraft health and safety because helicopters depend on the power train for propulsion, lift and control. Health and Usage Monitoring Systems (HUMS) capable of predicting impending transmission component failure for “on-condition” maintenance have the potential to decrease operating and maintenance costs and increase safety and aircraft availability. These systems employ “condition indicators” (CIs), typically calculated from vibration signatures, that are generated when a faulted component interacts with its operational environment. The CI must be correlated to a known failure mode to reliably detect the health of the system.

One method used to provide evidence that a HUMS can replace current maintenance practices required for “on-condition” maintenance is the performance of seeded fault tests. Seeded fault tests, within this paper, refer to initiating a known fault into a component to accelerate damage while monitoring its progression. The fault can be seeded by several different methods. The fault can be initiated by machining a fault into

the component prior to test. A component with an existing fault that was removed from a helicopter can be installed in a test rig for testing of its progression. The fault can also be forced to naturally occur through test design and operational conditions. For this analysis, the third method was used.

Damage progression “seeded fault” tests were performed in the NASA Glenn Spiral Bevel Gear Fatigue Test Rig to simulate failures of spiral bevel gears installed in a helicopter. Gear sets were tested until damage occurred on two or more gear or pinion teeth. Gear vibration, oil debris, torque and speed data were recorded with a research data acquisition system. Vibration and speed data were also recorded and processed with a helicopter HUMS system. A facility data acquisition system was used to monitor and record the operational conditions of the test rig. Tooth damage progression was documented with photographs of the gear teeth at periodic intervals throughout the test.

The objective of this work was to demonstrate the benefit of a software tool used to fuse the data generated from the three data acquisitions systems and the damage progression photos. The tool enabled correlation of the CI data with operational conditions the gear sets were exposed to during damage initiation and progression. Use of this tool will promote a better understanding of why gear vibration based CIs trend clearly with damage under some conditions but trend poorly for others, by determining which operational parameters and fault modes impact the effectiveness of each CI to indicate a gear fault.

**Test Facility:** Tests were performed in the Spiral Bevel Gear Fatigue Test Rig at NASA Glenn Research Center. A detailed description of this test facility is provided in references [1] and [2]. The Spiral Bevel Gear Fatigue Test Rig is illustrated in Figure 1. The facility operates as a closed-loop torque regenerative system, where the drive motor only needs enough power to overcome friction losses within the system. Two sets of spiral bevel gears are installed in the test rig and tested simultaneously. Facing the gearboxes, per Figure 1, the left gear set (pinion/gear) is referenced as left and the right gear set (pinion/gear) is referenced as right within the paper.

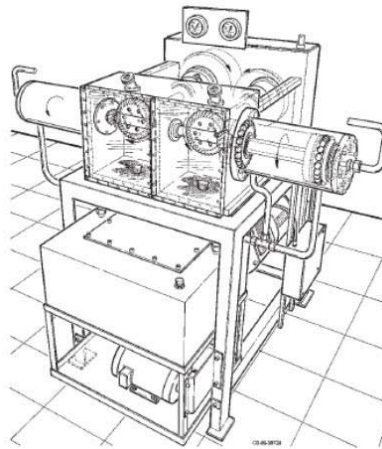


Figure 1: Spiral Bevel Gear Fatigue Test Rig.

Qualified helicopter transmission oil, AEROSHELL Turbine Oil 555, was used in the test rig during testing. Both gear sets are lubricated with oil jets pumped from an oil reservoir. The lubrication from the gearbox then exits the gearbox and flows through an inductance type in-line oil debris sensor, then past a magnetic chip detector. A strainer and a 3  $\mu\text{m}$  filter are located downstream of the oil debris (OD) sensor to capture any debris before returning to the sensor and gearbox.

**Data Acquisition and Instrumentation:** During these tests, three data acquisition systems were used. Vibration, oil debris, torque and speed data were collected once every minute with the NASA Glenn research data acquisition system, referred to as the Mechanical Diagnostic System Software (MDSS). Vibration and speed data were collected from a second set of sensors with a helicopter HUMS referred to as the Modern Signal Processing Unit (MSPU). Operational parameters were collected with a third system referred to as the Daytronic. These operational parameters included torque, speed, and right and left gearbox oil temperatures.

A non-contact rotary transformer shaft mounted torque sensor was used to measure torque during testing. Thermocouples were used to measure inlet and outlet oil temperatures. An inductance type oil debris sensor was used to measure the ferrous debris generated during fatigue damage to the gear teeth. The MDSS records the particle counts measured by the oil debris sensor, their approximate size and an approximate mass. The sensor measures the number of particles and their approximate size based on user defined particle size ranges or bins. Based on the bin configuration, the average particle size for each bin is used to calculate the cumulative mass by assuming the average particle size as a diameter spherical in shape and multiplying it by the density of steel. Chip indications from the magnetic chip detector, when the gap was closed with debris, were also measured.

For the MDSS system, accelerometers were installed on the right and left side of the test rig housing. Accelerometer frequency range is 0.7 to 20 KHz with a resonant frequency of  $\geq 70$  KHz. The MDSS accelerometers were mounted on the housing, radially and vertically with respect to the pinion, as shown in Figure 2. Facing the gearboxes, the left gear set (pinion/gear) and right gear set (pinion/gear) accelerometers were referenced as such in the MDSS system. Speed was measured with optical tachometers mounted on the left pinion shaft and left gear shaft to produce a separate once-per-rev tach pulse for the pinion and gears. Time synchronous averaging (TSA) of the vibration data collected from the left and right accelerometer is performed in the MDSS system for the pinions via the pinion tach pulse and the gears via the gear tach pulse.

For the MSPU system, accelerometers are also installed on the right and left side of the test rig. Accelerometer frequency range is 0.5 to 5 KHz with a resonant frequency of 26 KHz. A magnetic tachometer is installed on the right pinion and measures pinion pulses per tooth pass. This is used to calculate the TSA for both the pinion and the gear. The gear ratio is used to process the data at the correct speed for the gear. The MSPU accelerometers were mounted on the housing, in close proximity to the MDSS accelerometers, radially and vertically with respect to the pinion, as shown in Figure 2.

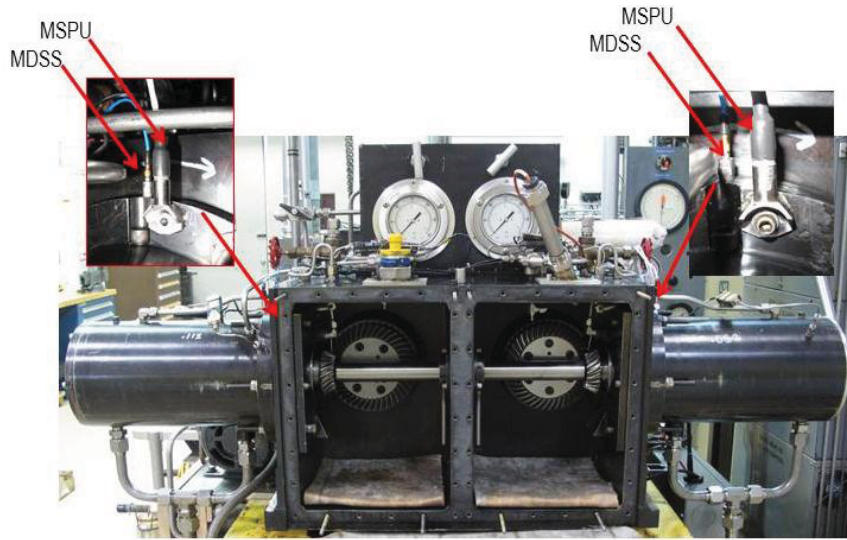


Figure 2: Location of Accelerometers.

Vibration data was collected at sample rates that provided sufficient vibration data for calculating time synchronous averaged data (TSA). TSA refers to techniques for averaging vibration signals over several revolutions of the shaft, in the time domain, to improve signal-to-noise ratio [3]. Using a once-per-revolution signal or tachometer, the vibration signal is interpolated into a fixed number of points per shaft revolution. Vibration signals synchronous with the shaft speed intensify relative to non-periodic signals which become weaker.

Since helicopter gears generate vibration signals synchronous with gear rotational speed, most current helicopter gear CIs are calculated from TSA data. Many CIs are based on statistical measurements of vibration energy. Signal processing techniques used to extract useful information to calculate a gear CI from the vibration signal are discussed in detail in reference [4]. Some gear CIs are calculated directly from the TSA signal, such as Root Mean Square (RMS). Some are calculated from the TSA converted to the frequency domain, such as Sideband Index (SI). Some convert the TSA signal to the frequency domain, filter specific frequencies, convert it back to the time domain, then calculate a statistical parameter from this data [3 to 5].

Figure 3 illustrates the information used to calculate the TSA for the right gear and pinion. Using the sample rate of 200 KHz for 1 sec duration and the speed of both shafts, the number of TSA revolutions averaged for each acquisition is determined. To calculate the TSA, the accelerometer data is divided into segments equivalent to 1 revolution of the shaft. Each segment is then linearly interpolated into equal numbers of points that have been rounded down to a power of two. A power of two is used because it eases the future use of the Fast Fourier Transform (FFT) to transform the TSA to the frequency domain. Per Figure 3, the right accelerometer raw data is plotted in the top plot. The two lowest plots are the TSA signal calculated from the 1/rev and vibration data for the right gear and pinion. Pulses from the 41 tooth gear and the 19 tooth pinion can easily be seen within these two plots.



TSA Info	Pinion	Gear
Test Gear Teeth	19	41
Max Speed (RPM)	7553	3500
Max Speed (Hz)	126	58
Gear Mesh (Hz)	2392	2392
Sample rate	200000	200000
Sample Duration (sec)	1	1
Revs per Acq	126	58
TSA int. points/rev	1024	2048

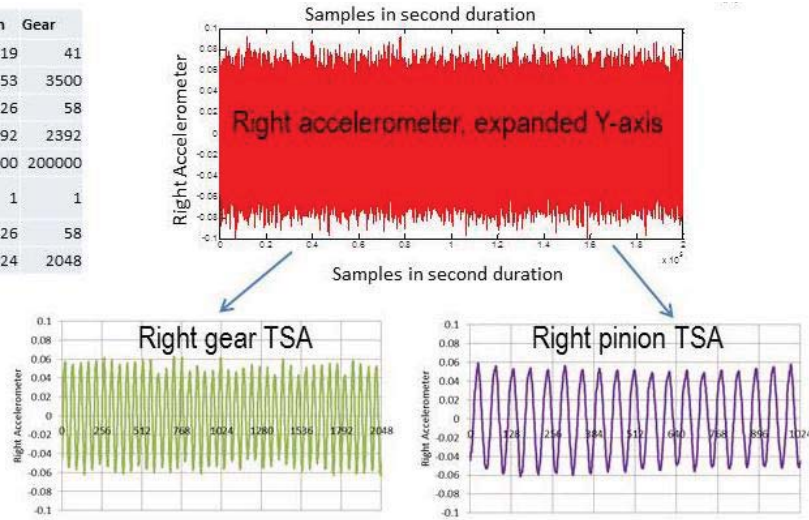


Figure 3: Information Used to Calculate TSA.

**Test Gear Sets:** The gears were made from a steel alloy CEVM 9310, carburized, hardened and ground. The test gears are the gear sets (pinion/gear) installed on the left side of the rig. The slave gears are the gear sets installed on the right side of the rig. The right gear sets are superfinished to decrease wear rates and increase their life. The gear sets have a 6.4 in. diametral pitch, 20° pressure angle, 25° spiral angle, 0.94 in. face width and a 2.15 gear ratio. The gears have 41 teeth and the pinions have 19 teeth. The test gears were designed to operate at a gear speed of 3500 rpm, gear torque of 8000 in.-lbs., pinion speed of 7553 rpm, pinion torque of 3707 in.-lbs. and 240 to 265 °F inlet oil temperatures with an American Gear Manufacturers Association (AGMA) calculated contact stress of 237 ksi.

**Test Description:** For this study, two left gear sets were tested at a gear speed of 3500 rpm and pinion speed of 7553 rpm. At the start of each test, a run-in was performed for a minimum of 1 hour at 4000 in.-lbs. gear torque/3500 rpm gear speed and 1854 in.-lbs. pinion torque/7553 rpm pinion speed. Then the gear torque was increased to 8000 in.-lbs. and pinion torque was increased to 3707 in.-lbs. for the remainder of the test. Contact cycles accumulated at a rate of 210,000 per hour for the gear and 453,180 per hour for the pinion. At completion of the run-in, inspection photos were taken of the left and right gear and pinion teeth. Inspection photos were also taken periodically throughout the test to document damage progression to the gear teeth.

The failure modes to be investigated for this study were defined by class (contact fatigue), general mode (macro pitting) and degree (progressive) per American Gear Manufacturers Association (AGMA) standards for gear wear terminology [6]. Using [6] for tooth damage terminology, a numbering scheme [7] was developed to streamline the identification of gear damage. Table 1 illustrates the types of damage observed during these tests. The tests ran until macro pitting/spalling larger than 1 mm in diameter covered a significant area of two or more gear or pinion tooth surfaces. Definitions for tooth surface pitting modes [6] are summarized as follows:

- Initial—Pits less than 1 mm in diameter.

- Progressive—Pits in different shapes/sizes greater than 1 mm in diameter.
- Flake—Pits that are shallow thin flakes.
- Spalling—Pits that cover tooth contact surfaces that exceed progressive pitting.

During test 2, scuffing occurred prior to contact fatigue damage. Scuffing causes transfer of metal from one tooth surface to another. This failure class is also listed in Table 1.

Table 1: Numbering Scheme for Nomenclature of Gear Failure Modes [6].

Class	General Mode	Specific Mode or Degree
2.0 Scuffing	2.1 Scuffing	2.1.1 Mild
		2.1.2 Moderate
		2.1.3 Severe
4.0 Contact Fatigue	4.1 Subcase Fatigue	
	4.2 Micropitting	
	4.3 Macropitting	4.3.1 Initial
		4.3.2 Progressive
		4.3.3 Flake
		4.3.4 Spall

**Software Tool:** Many factors can affect the gear CI's ability to respond to tooth damage through vibration response. The response of the accelerometer to a specific fault can depend on the sensor specifications, the signal processing of the raw signal, mounting and its location. The CI method of calculation, operational conditions and type of failure mode can also affect its response.

Assessing whether a change in any particular condition indicator was due solely to a change in damage level, a change in operating condition or some combination of both was a challenge due to three data acquisitions systems with different measured parameters and acquisition rates. To assess the relationship between the different parameters, a software tool was developed to fuse the three systems. The tool provided a means to analyze the data generated during gear damage initiation and progression from the three data acquisitions systems and the damage progression photos. This software tool enables fusing the information from the three data acquisition systems (MDSS, MSPU and Daytronic) and the damage modes. The data can be plotted and analyzed separately or correlated together. The tool also provides a means for inputting damage levels for further correlation. Summarized statistical parameters for CIs and operational conditions can be calculated and exported into tables. A screen shot of the tool is shown in Figure 4.

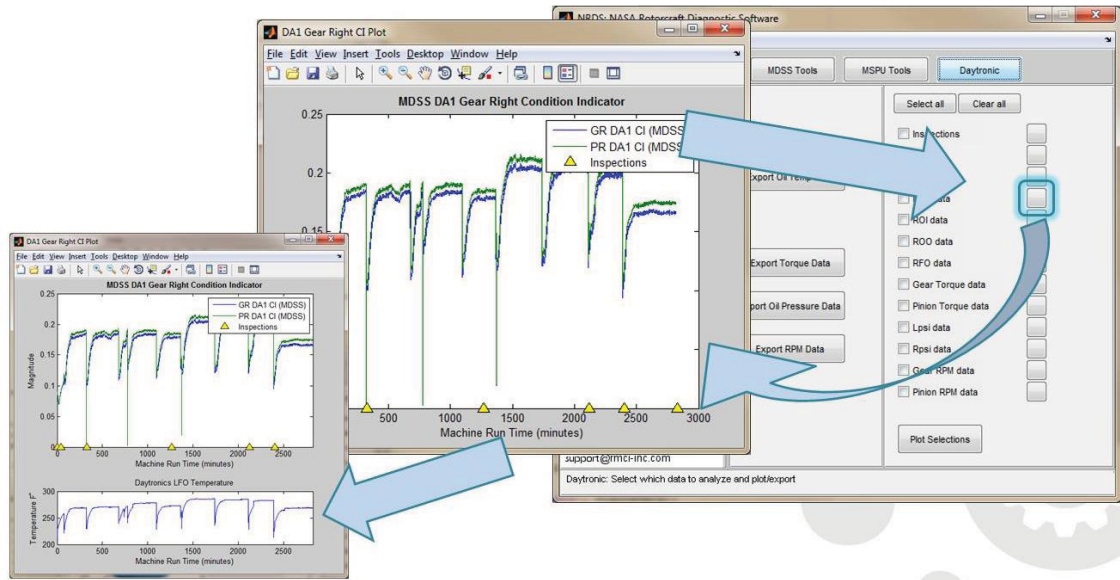


Figure 4: Data Fusion Tool.

**Tool Demonstration:** Summaries of the tools capabilities on the Spiral Bevel Gear Fatigue Test Rig test data will be discussed in the following sections. These summaries will include plots of CIs from both the MDSS and MSPU systems, debris generated and gear torque. Note that the CIs for each component are identified as GL (gear left), GR (gear right), PL (pinion left) and PR (pinion right). Torque was measured in inch-pounds and debris generated was measured in milligrams. Tooth damage photos for the gear and pinion during inspection intervals were converted to a damage scale per Table 2. User defined damage scales of zero through three identify gear tooth condition. The damage scales are followed by a user defined letter that indicates the classification of the damage. The scales are used to provide a damage level indication on the x-axis of the plots via green, yellow or red triangles. For the tests to be discussed, 2a indicated macropitting on one tooth, 3a indicated macropitting initially observed on two or more teeth, and 3b indicated the pitting area increased on the tooth surface between inspection intervals.

Table 2: Damage Scales.

Damage Scale	Gear Condition	Indication
0	New	●
1[a-z]	Minor Wear	▲
2[a-z]	Minor Damage	▲
3[a-z]	Significant Damage	▲

For test 1, contact fatigue damage was first observed on left pinion tooth 10 at run time 2119 min. Damage was observed on a second tooth, left pinion tooth 13, at run time 2402 min. The size of the spall increased on left pinion tooth 13 at run time 2402 min. Photographs of damage progression on the two pinion teeth are shown in Figure 5. Table 3 lists the inspection intervals and damage scales observed during testing. The CIs evaluated will be discussed in the following section.

Left Pinion  
tooth 10

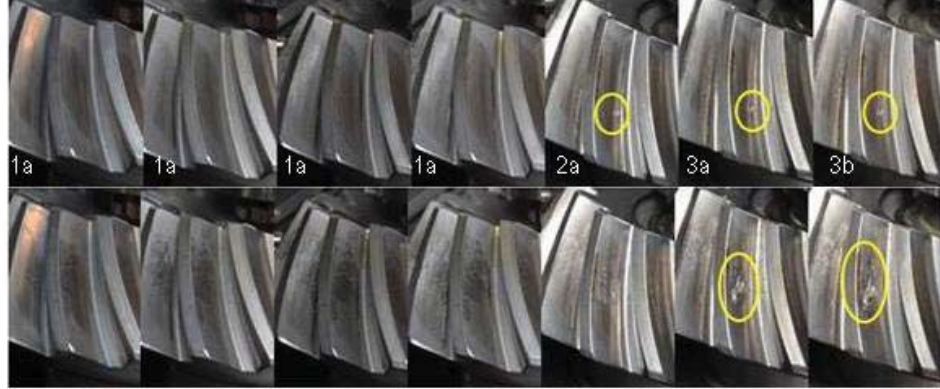


Figure 5: Left Pinion Tooth Damage.

Table 3: Test 1 Inspection Intervals and Observed Damage Scales.

Date	Run Time (min.)	Damage Scale
2013-03-21	1	1a
2013-03-22	76	1a
2013-03-26	324	1a
2013-04-02	1370	1a
2013-04-11	2119	2a
2013-04-15	2402	3a
2013-04-17	2833	3b

**Condition Indicators:** FM4 is one CI used to indicate gear tooth damage. Figure 6 is a block diagram of the steps required to calculate FM4 (Figure of Merit 4), a common vibration algorithm used in commercial HUMS [3].

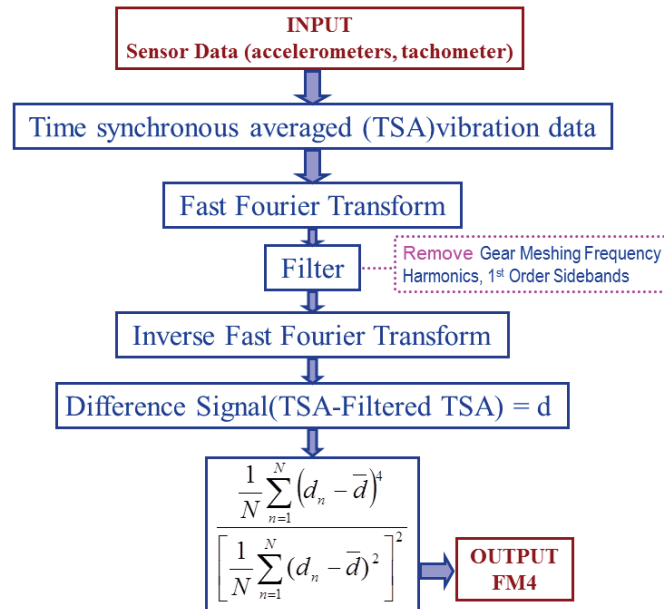


Figure 6: FM4 Calculation.



Figure 7 contains plots of FM4, oil debris, gear torque, gear speed, and left and right side of gearbox oil output temperatures. FM4 values for the left pinion increased significantly when damage was observed on two left pinion teeth. Oil debris mass also increased as damage progressed on the pinion teeth. FM4 did not appear to be significantly affected by the varying operational parameters (gear torque, gear speed and output oil temperatures).

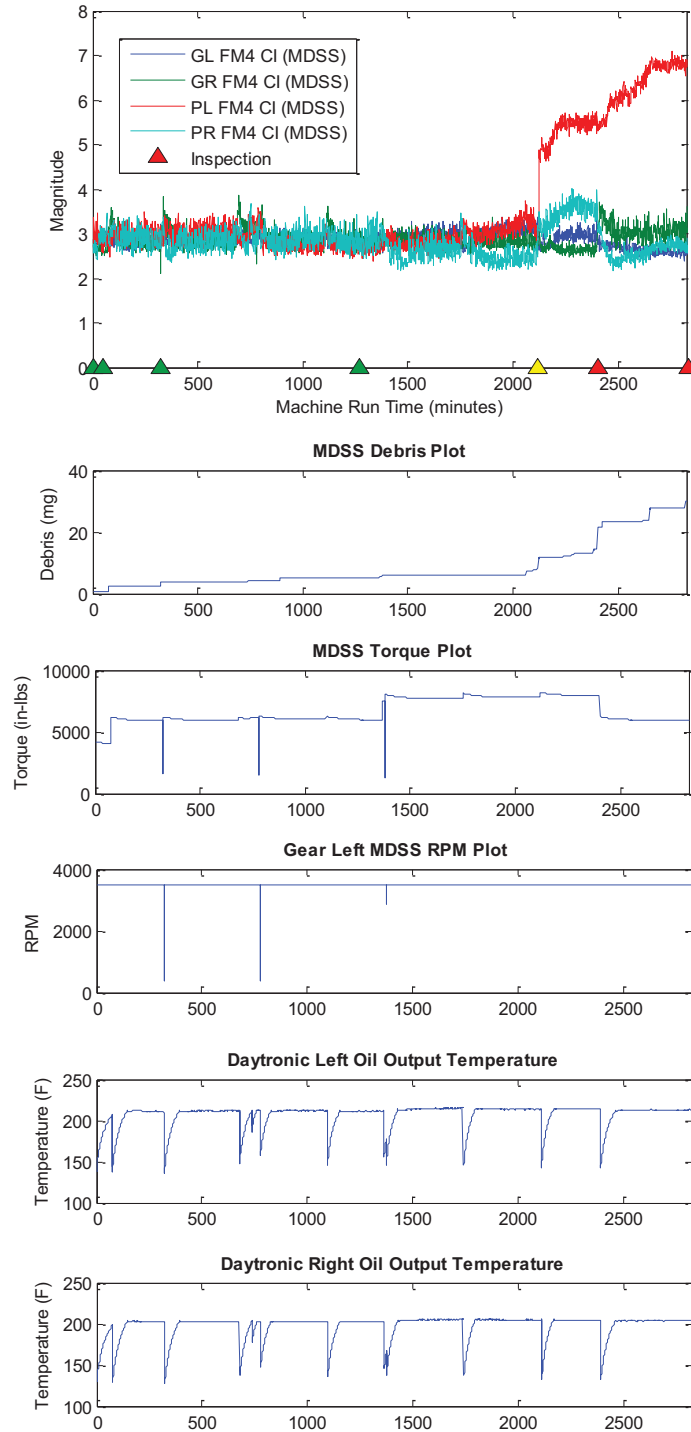


Figure 7: FM4 and Operational Parameters.

RMS or DA1 is another CI used to indicate gear tooth damage. Figure 8 is a block diagram of the steps required to calculate RMS.

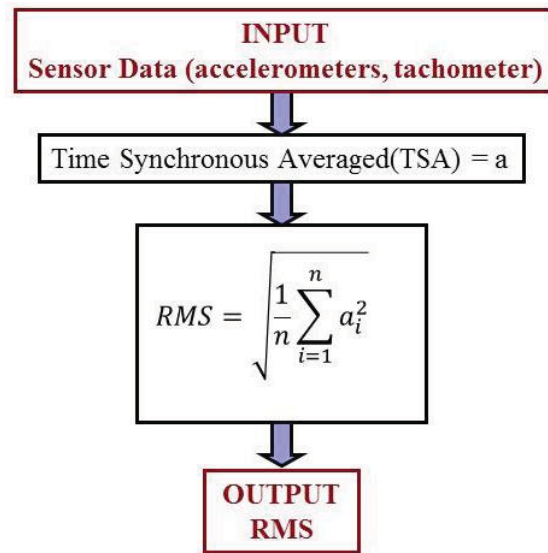


Figure 8: RMS Calculation.

Figure 9 contains plots of RMS, oil debris, gear torque, gear speed, and left and right oil output temperatures. RMS values for the *right* side were significantly higher than the left and were sensitive to torque and oil outlet temperature transients. RMS values for the *left* side were sensitive to torque. However, once damage was observed on two pinion teeth, the RMS value for the left pinion did not drop when torque decreased.

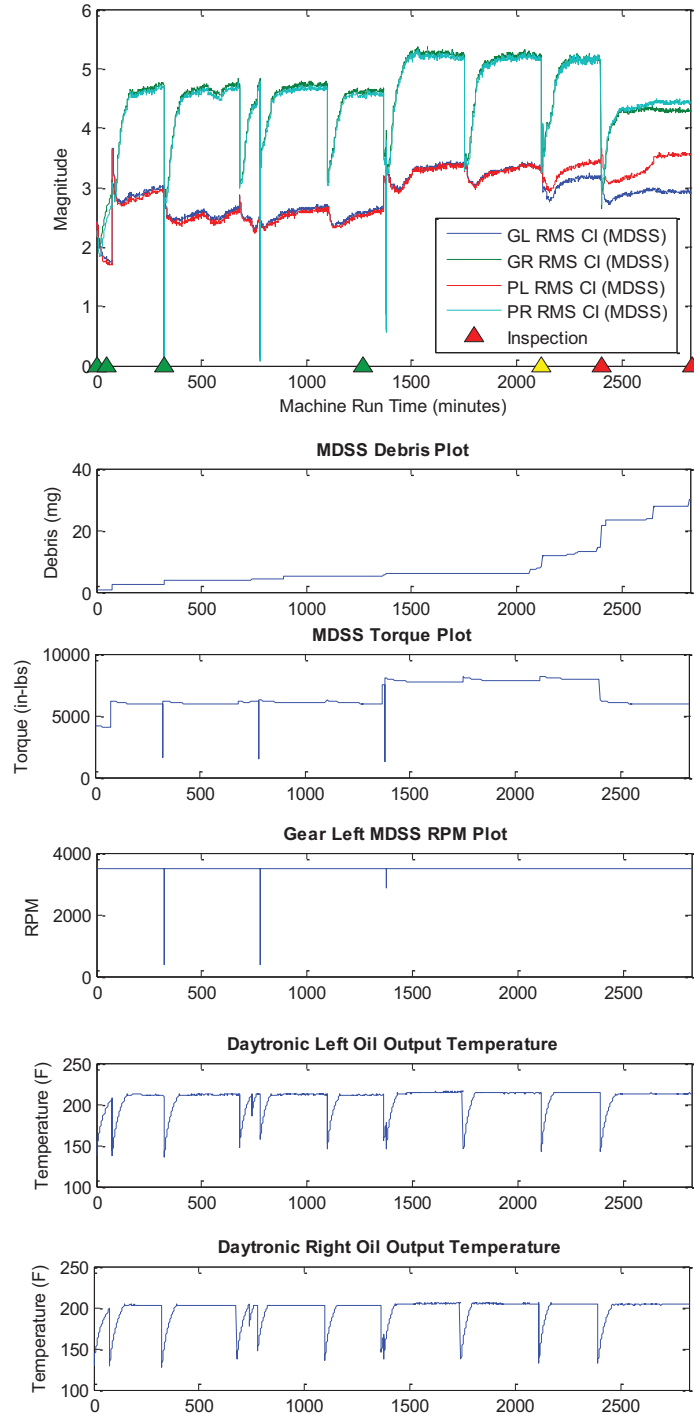


Figure 9: RMS and Operational Parameters.

Sideband index (SI) is another CI used to indicate gear tooth damage. SI is a frequency domain based CI. The CI value is an average value of sideband amplitudes about the fundamental gear mesh frequency. All gears generate a dominant gear mesh (GM) frequency in the vibration signature due to each tooth impacting the gear it is driving as the pinion and gear mesh. The gear (or pinion) mesh frequency is equal to the number of teeth multiplied by its speed. The number of sidebands included in the calculation of the sideband CI can vary with different health monitoring systems. Averages of  $\pm 1$  (SI1) and  $\pm 3$  (SI3) were used for this analysis. Figure 10 is a block diagram of the steps required to calculate SI1.

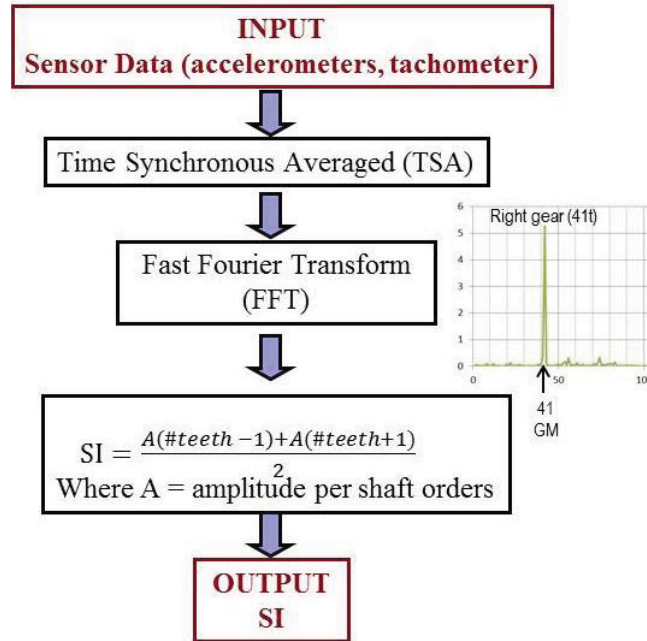


Figure 10: SI1 calculation.

Figure 11 contains plots of the average of  $\pm 1$  sideband (SI1), oil debris, gear torque, gear speed, and left and right oil outlet temperatures. SI1 values for the *right* side were sensitive to torque and oil outlet temperature transients. SI1 values for the *left* side were not sensitive to torque. SI1 values for the left pinion increased significantly when damage was observed on two left pinion teeth.

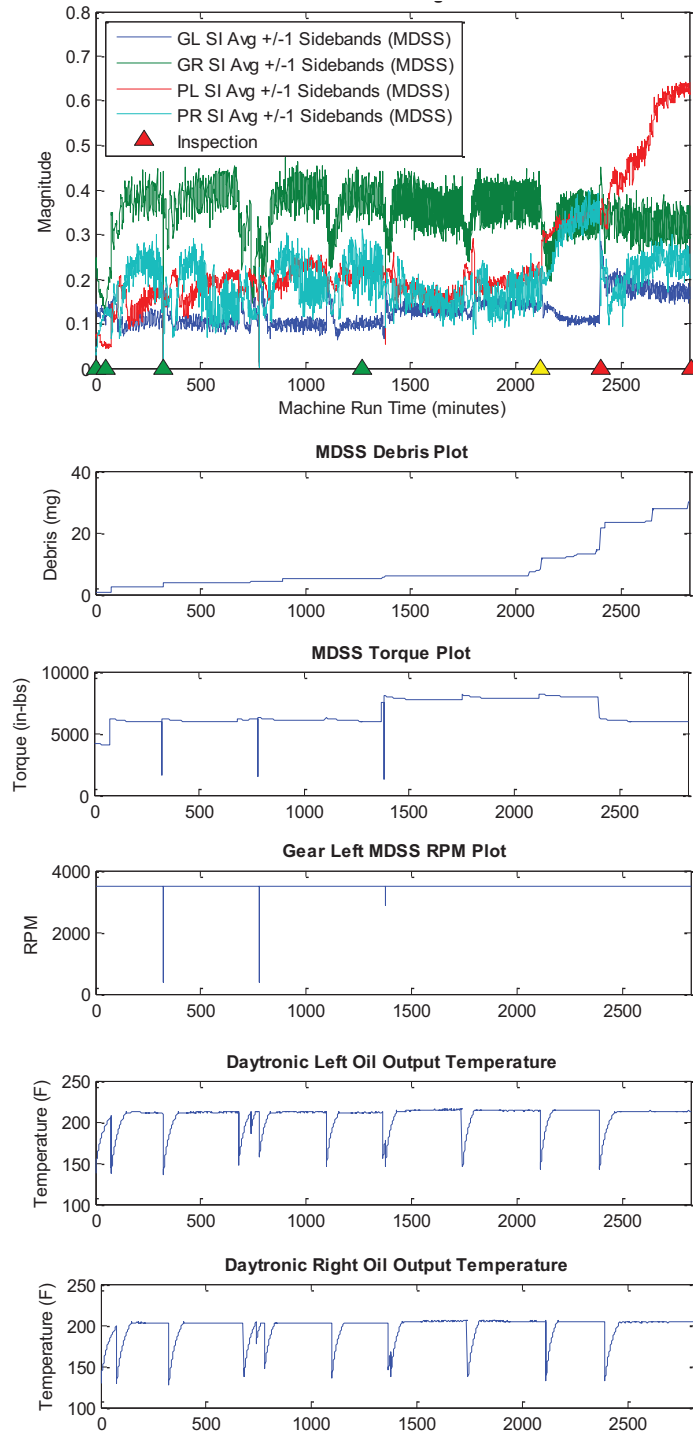


Figure 11: SI1 and Operational Parameters.



CIs calculated separately from the two different health monitoring systems were compared to determine if system differences affected CI response. Figures 12 and 13 contain plots of the average of  $\pm 1$  sideband (SI1) and average of  $\pm 3$  sidebands (SI3) for the MDSS and MSPU systems. Figure 14 contains plots of RMS, referred to as DA1, in the MDSS system for the MDSS and MSPU systems. Figure 15 contains plots of FM4 for the MDSS and MSPU systems. Although data was collected more frequently with the MDSS system, both systems trended well together.

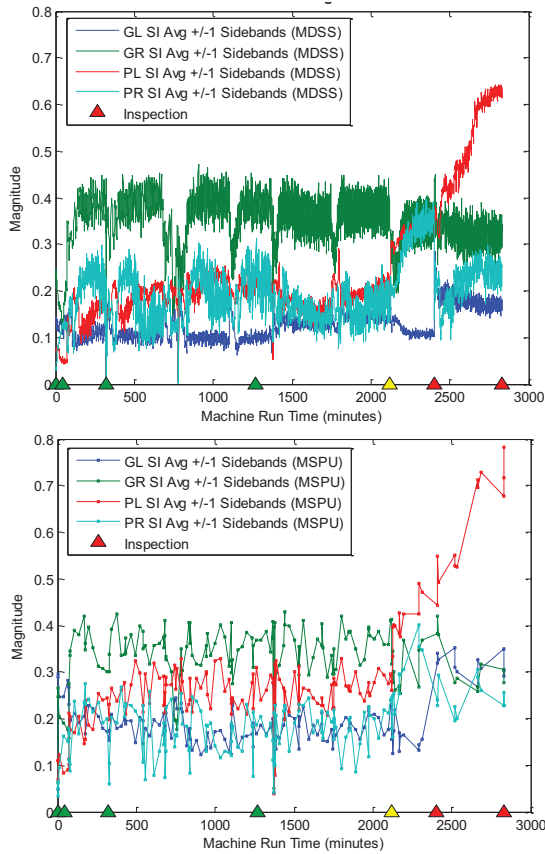


Figure 12: MDSS and MSPU SI1.

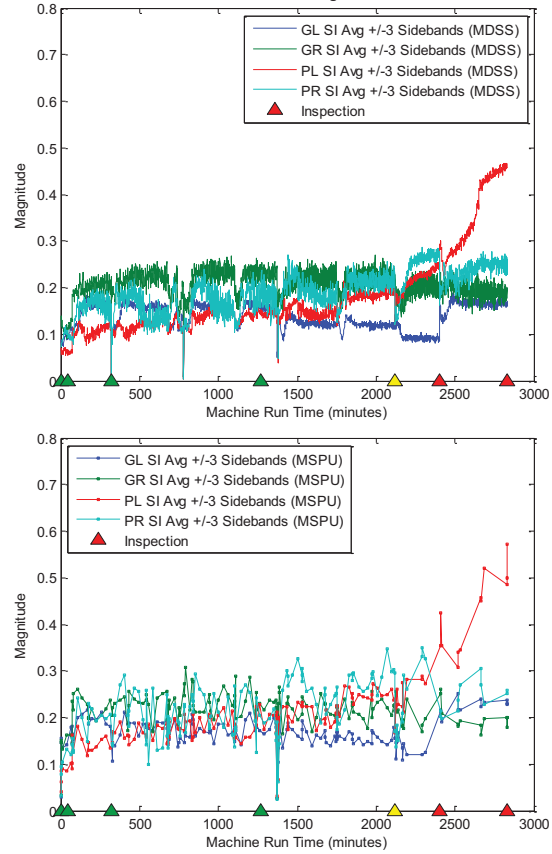


Figure 13: MDSS and MSPU SI3.

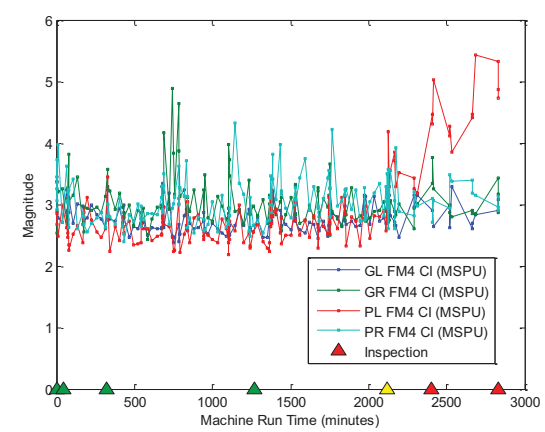
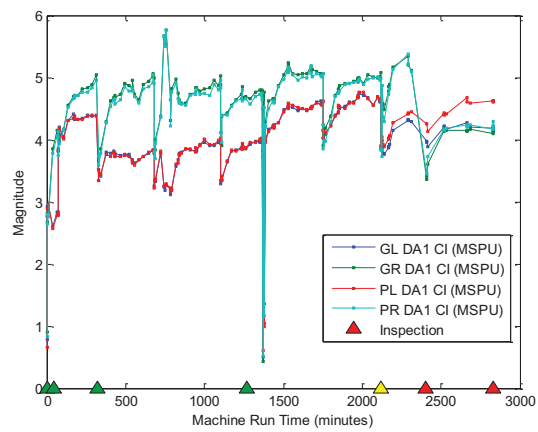
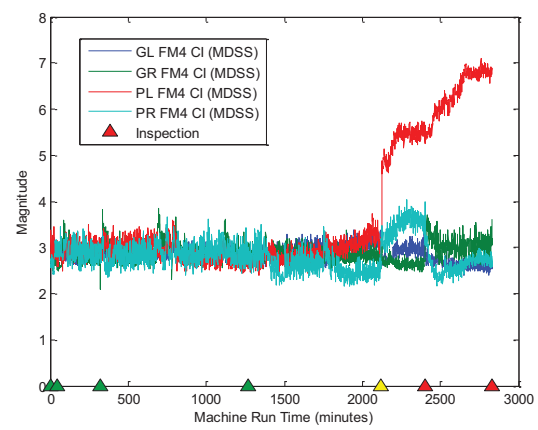
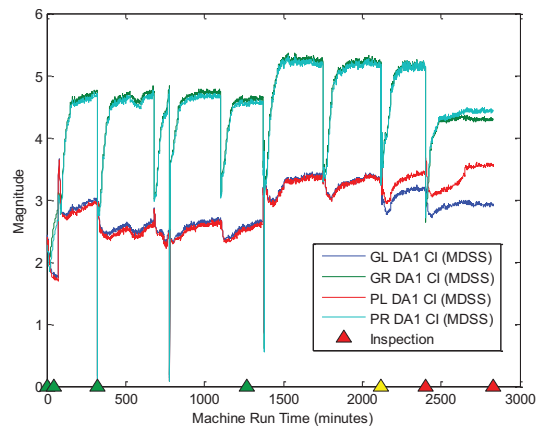


Figure 14: MDSS and MSPU DA1.

Figure 15: MDSS and MSPU FM4.

The software tool also generates tables of statistical parameters within each inspection interval for comparison. Table 4 summarizes the mean, standard deviation and RMS values calculated from MDSS within each inspection interval for FM4, RMS, SI1, and SI3. The cells highlighted identify the timeframe when damage was observed on the left pinion teeth (PL). During the inspection interval when damage was observed on two or more pinion teeth, run time 2120 to 2403 min, mean values for FM4 and SI1 were higher for the left pinion than the other three components monitored.

Table 4: RMS, FM4 and SI Statistical Parameters for Test 1.

<b>MDSS RMS</b>	Mean	STDEV	RMS	Mean	STDEV	RMS	Mean	STDEV	RMS	Mean	STDEV	RMS
Inspection	GL	GL	GL	GR	GR	GR	PL	PL	PL	PR	PR	PR
1 - 43	2.05	0.22	2.06	2.26	0.14	2.26	2.00	0.23	2.01	2.09	0.15	2.09
43 - 325	2.77	0.42	2.80	4.15	0.78	4.22	2.71	0.42	2.74	4.08	0.81	4.16
325 - 1266	2.53	0.13	2.53	4.40	0.49	4.43	2.48	0.13	2.48	4.35	0.48	4.37
1266 - 2120	3.18	0.26	3.19	4.93	0.53	4.96	3.16	0.27	3.17	4.87	0.54	4.90
2120 - 2403	3.08	0.13	3.08	4.85	0.51	4.88	3.28	0.15	3.28	4.83	0.52	4.86
2403 - 2833	2.91	0.07	2.91	4.19	0.30	4.20	3.35	0.19	3.36	4.28	0.31	4.29
<b>MDSS FM4</b>	Mean	STDEV	RMS	Mean	STDEV	RMS	Mean	STDEV	RMS	Mean	STDEV	RMS
Inspection	GL	GL	GL	GR	GR	GR	PL	PL	PL	PR	PR	PR
1 - 43	2.83	0.11	2.83	2.68	0.10	2.68	2.95	0.16	2.96	2.74	0.20	2.75
43 - 325	2.80	0.10	2.80	2.88	0.21	2.88	2.96	0.17	2.97	2.91	0.19	2.92
325 - 1266	2.88	0.09	2.88	2.91	0.22	2.92	2.90	0.22	2.91	2.87	0.20	2.88
1266 - 2120	2.97	0.14	2.97	2.84	0.13	2.84	2.92	0.23	2.92	2.61	0.24	2.62
2120 - 2403	2.91	0.13	2.91	2.67	0.10	2.67	5.29	0.40	5.31	3.47	0.23	3.48
2403 - 2833	2.65	0.10	2.65	3.07	0.20	3.07	6.37	0.46	6.39	2.62	0.19	2.63
<b>MDSS <math>\pm 1</math> SI</b>	Mean	STDEV	RMS	Mean	STDEV	RMS	Mean	STDEV	RMS	Mean	STDEV	RMS
Inspection	GL	GL	GL	GR	GR	GR	PL	PL	PL	PR	PR	PR
1 - 43	0.1265	0.0079	0.1268	0.1799	0.0324	0.1827	0.0649	0.0102	0.0656	0.0844	0.0278	0.0888
43 - 325	0.1098	0.0202	0.1116	0.3466	0.0768	0.3550	0.1370	0.0420	0.1433	0.1933	0.0548	0.2009
325 - 1266	0.1064	0.0230	0.1089	0.3625	0.0584	0.3671	0.1978	0.0269	0.1996	0.1801	0.0519	0.1875
1266 - 2120	0.1311	0.0175	0.1323	0.3646	0.0427	0.3670	0.1900	0.0267	0.1918	0.1709	0.0388	0.1752
2120 - 2403	0.1164	0.0179	0.1177	0.3261	0.0477	0.3295	0.3265	0.0254	0.3275	0.2991	0.0596	0.3049
2403 - 2833	0.1831	0.0215	0.1843	0.3275	0.0350	0.3293	0.5100	0.0967	0.5191	0.2190	0.0394	0.2225
<b>MDSS <math>\pm 3</math> SI</b>	Mean	STDEV	RMS	Mean	STDEV	RMS	Mean	STDEV	RMS	Mean	STDEV	RMS
Inspection	GL	GL	GL	GR	GR	GR	PL	PL	PL	PR	PR	PR
1 - 43	0.0871	0.0076	0.0874	0.1134	0.0108	0.1139	0.0635	0.0043	0.0637	0.0970	0.0130	0.0978
43 - 325	0.1486	0.0271	0.1511	0.1914	0.0319	0.1940	0.1020	0.0193	0.1038	0.1504	0.0307	0.1535
325 - 1266	0.1494	0.0189	0.1506	0.2162	0.0260	0.2177	0.1284	0.0166	0.1295	0.1619	0.0324	0.1651
1266 - 2120	0.1251	0.0163	0.1261	0.2168	0.0214	0.2179	0.1610	0.0217	0.1625	0.1972	0.0272	0.1991
2120 - 2403	0.0952	0.0116	0.0959	0.1979	0.0207	0.1990	0.2151	0.0254	0.2166	0.2381	0.0436	0.2421
2403 - 2833	0.1645	0.0118	0.1649	0.1961	0.0159	0.1967	0.3585	0.0768	0.3666	0.2364	0.0202	0.2373

For test 2, a different failure mode occurred when full load was applied after run-in. This caused scuffing to occur on the left pinion and gear teeth. Scuffing is not a fatigue failure mode. This failure mode causes the transfer of metal between the meshing teeth and does not cause debris to be generated. Photographs of the damage are shown in Figure 16. The first two photos are at test start and after run-in. The scuffing occurred when full load was applied at reading 70. This accelerated the contact fatigue failure mode as shown in the photographs of left pinion teeth 2, 4, 8, 14, 18, and 19. A representative photo of all left gear teeth damage is shown for left gear tooth 3. At reading 214, macro pitting was observed on six pinion teeth.

Plots of RMS for all four components and SI1 and SI3 averages for the left pinion and gear are shown in Figure 17. RMS was a good indicator of the left pinion damage and trended as damage increased. Note the increase in debris at reading 180 indicates the pitting initiation on the pinion teeth. Both gear sideband indexes slightly increased with scuffing, then slightly decreased with pitting.

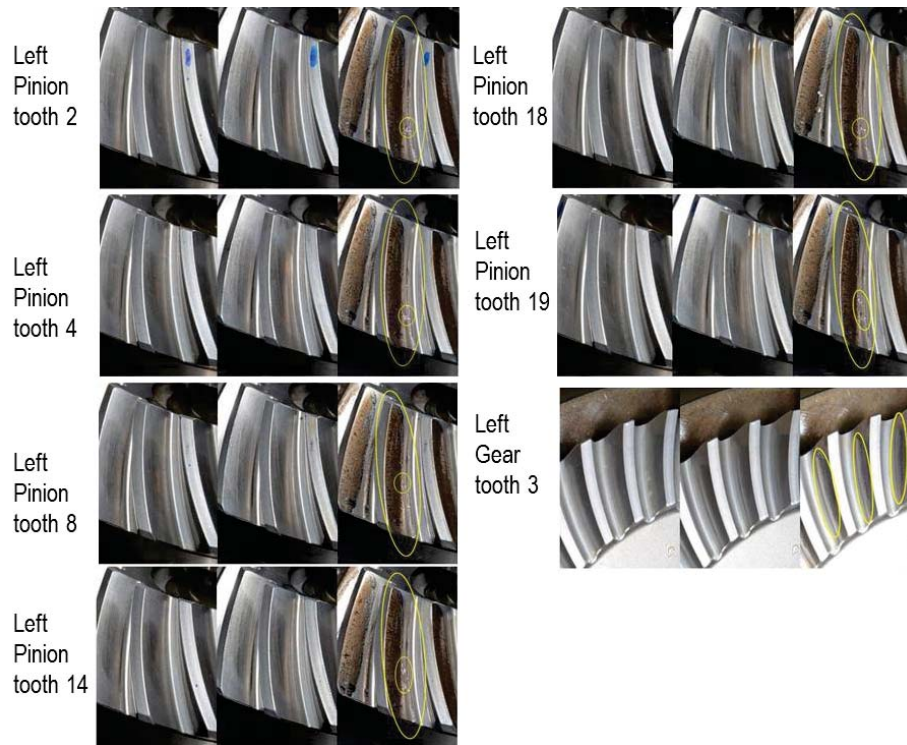


Figure 16: Pinion and Gear Teeth Damage.

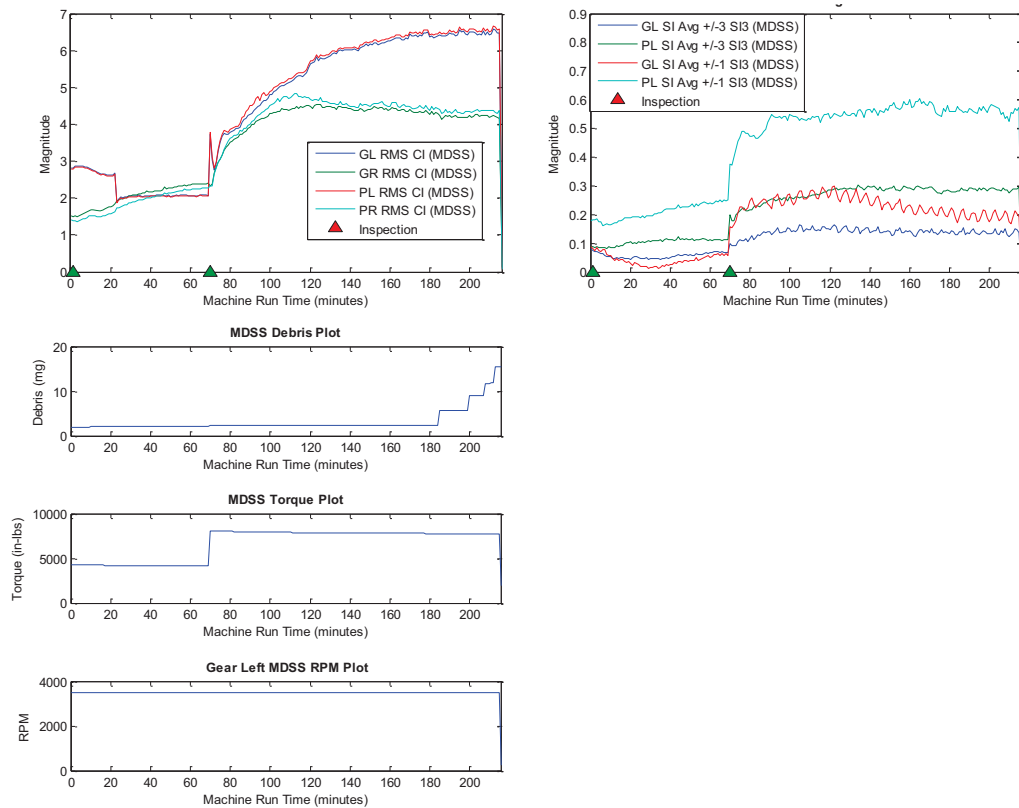


Figure 17: MDSS RMS and SII and SI3 Averages.

**Correlation Analysis:** To evaluate the relationship between CIs and operational conditions, the software tool allows the user to select parameters to correlate using the Pearson Correlation Coefficients ( $r$ ). Correlation coefficients measure the strength and direction of the linear relationship between two parameters [8]. Correlation coefficients are calculated by dividing the covariance of the two variables by the product of their standard deviations. Its value ranges between  $-1$  and  $+1$ . A perfect linear relationship between two parameters will have a correlation coefficient of  $1$  or  $-1$ . Positive values indicate both parameters increase. Negative values indicate as one parameter increases, the other decreases. A value close to zero indicates no linear relationship between the two parameters. Hypothesis tests can be used to assess the significance of the relationship between the two parameters; however, a good rule of thumb is that values greater than  $0.8$  indicate a strong correlation and values less than  $0.5$  indicate a weak correlation.

When comparing data from several different data acquisition systems collected at varying acquisition intervals, a method to align the timestamps and fill in the gaps of data for the systems recorded at a lower acquisition rates must be defined. This is required when applying statistical methods or data mining techniques to correlate relationships between variables across the systems. The MDSS and Daytronic systems acquired data once per minute. The MSPU system acquired data once per 30 min. Since the MDSS, MSPU and Daytronic systems collected data at varying acquisitions intervals, the software tool provided three methods to align timestamps and fill in data gaps: (1) Nearest Neighbor; (2) Linear Interpolation, and (3) Filtered Spline. The linear interpolation method was used in the presented analysis. For this method, data points from the smaller data set are truncated to fall within the time range of the larger data set and timestamps from the smaller data set are used to linearly interpolate new values for the larger data set.

Figure 18 illustrates the linear interpolation method applied to the left pinion (PL) average SII for the MDSS and MSPU data set previously plotted in Figure 12. The plot on the top left is the actual data. The plot on the right is the linear interpolated data with a correlation coefficient of  $0.94$ . The bottom plot compares the left pinion MSPU SII values to the MDSS SII values. Figures 19 to 24 are plots of CIs versus oil outlet temperatures and torques. The  $r$  values for the two plotted parameters are shown in red.

Figure 19 compares the RMS values for the right gear and right pinion to the right oil outlet (ROO) temperatures measured on the right side of the test rig. RMS values for the left gear and pinion are compared to the left oil outlet (LOO) temperatures. The plots indicate a strong positive correlation with right oil outlet temperatures and right gear and pinion RMS values ( $0.78$  and  $0.79$ ). Figure 20 compares the RMS values for the right gear, right pinion, left gear and left pinion to the applied torque. All four RMS values correlate to positive torque values. However, the left gear indicates a significantly stronger correlation ( $0.82$ ) than the other three RMS values.



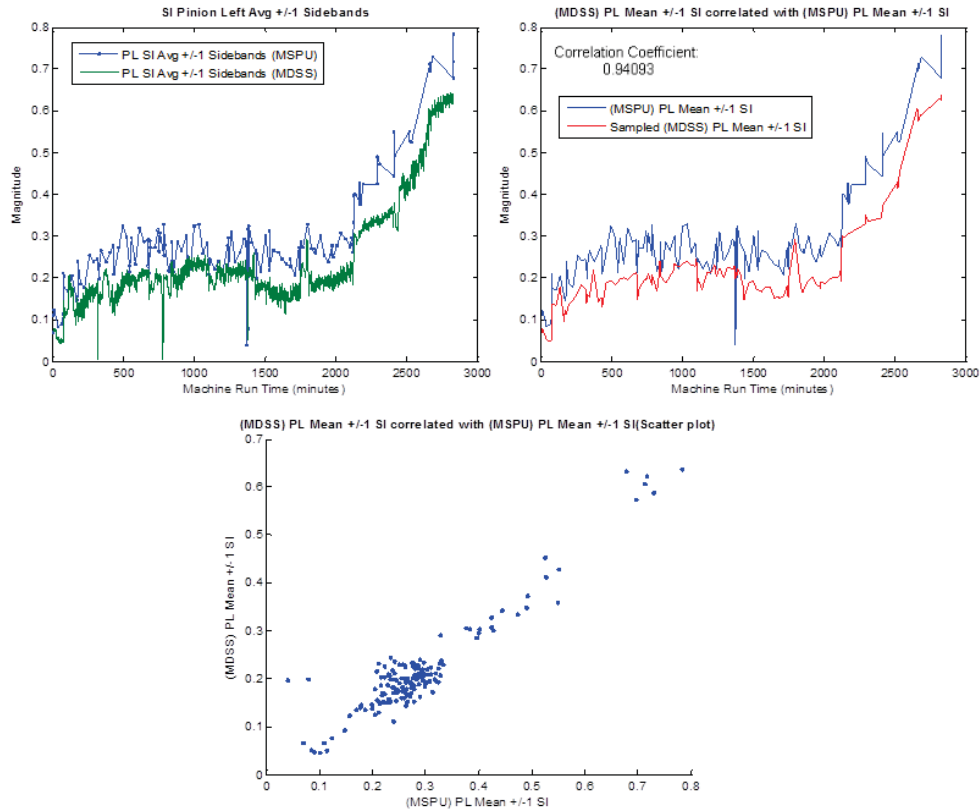


Figure 18: Linear Interpolation of MDSS and MSPU SI1.

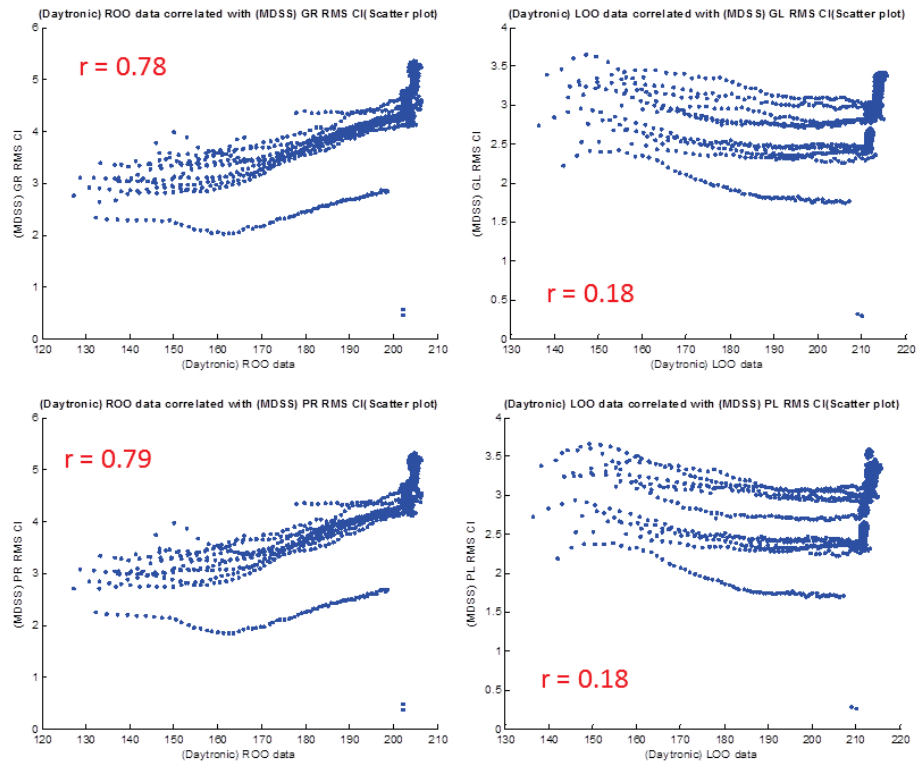


Figure 19: Correlation Between RMS and Outlet Oil Temperatures.

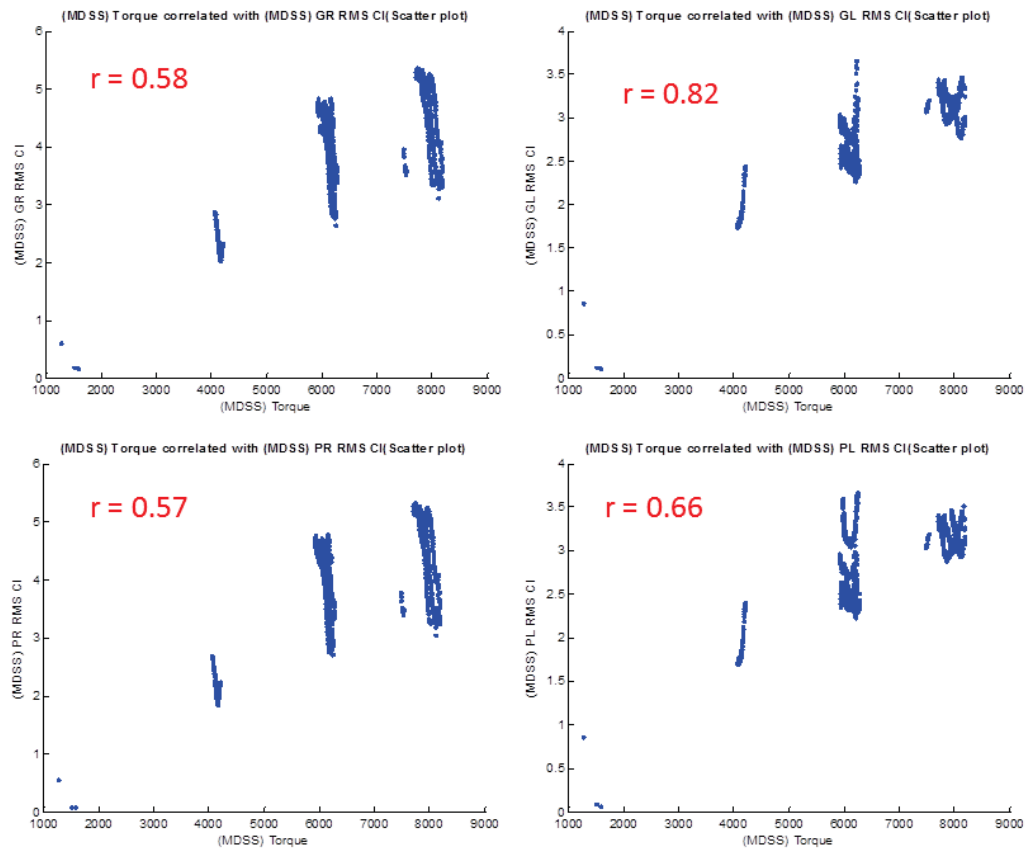


Figure 20: Correlation Between RMS and Torques.

Figure 21 compares the FM4 values for the right gear and right pinion to the oil outlet temperatures measured on the right side of the test rig. FM4 values for the left gear and pinion are compared to the left oil outlet temperatures. The plots indicate a weak correlation between FM4 and oil outlet temperatures for all four components. Figure 22 compares the FM4 values for the right gear, right pinion, left gear and left pinion to the applied torque. All four FM4 values indicate a weak correlation to torque. Note the plot of FM4 for the left pinion in the bottom right hand corner. The separation of FM4 values at 6000 and 8000 in.-lbs. are an indication of the larger FM4 values due to pinion tooth damage.

Figure 23 compares the SI1 values for the right gear and right pinion to the oil outlet temperatures measured on the right side of the test rig. SI1 values for the left gear and pinion are compared to the left oil outlet temperatures. All four SI1 values indicate a weak correlation with oil outlet temperatures. Figure 24 compares the SI1 values for the right gear, right pinion, left gear and left pinion to the applied torque. All four SI1 values indicate a weak correlation with torque.

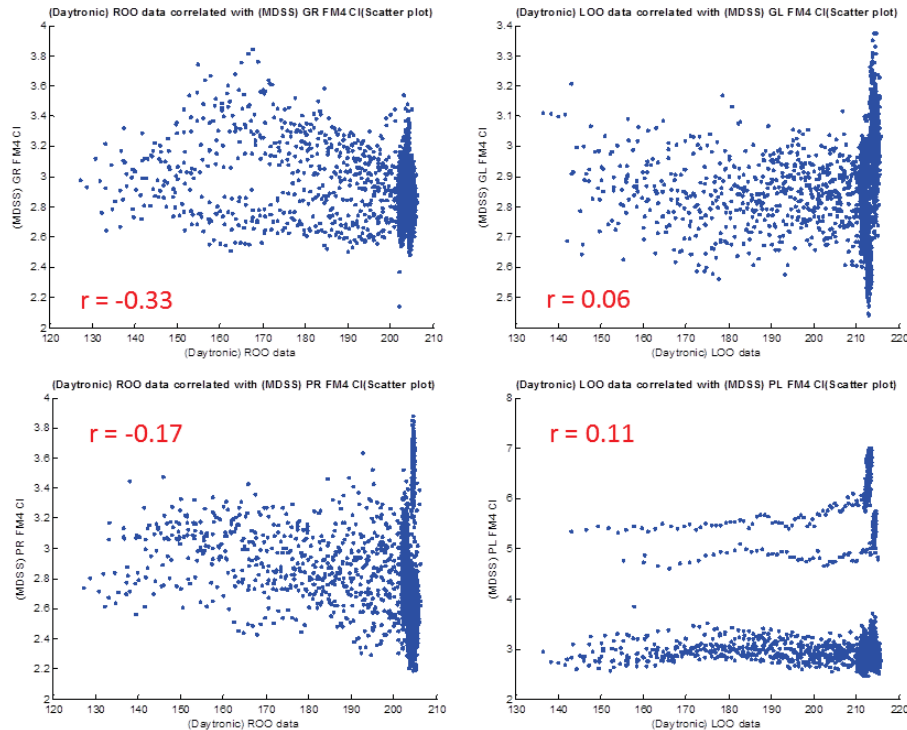


Figure 21. Correlation Between FM4 and Outlet Oil Temperatures.

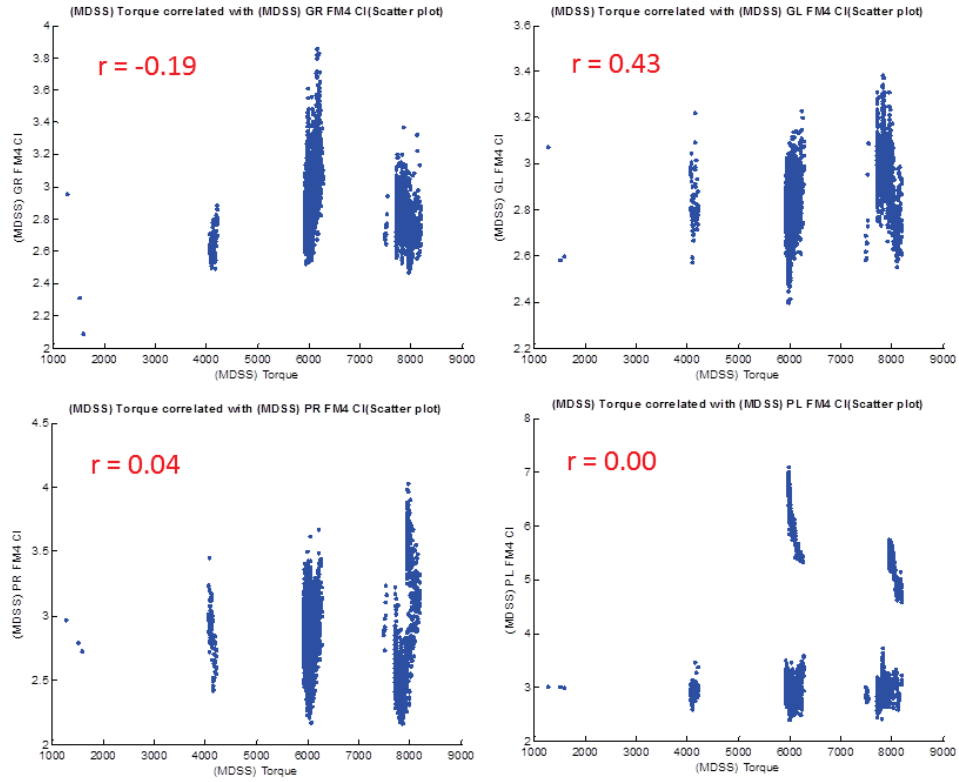


Figure 22: Correlation Between FM4 and Torques.

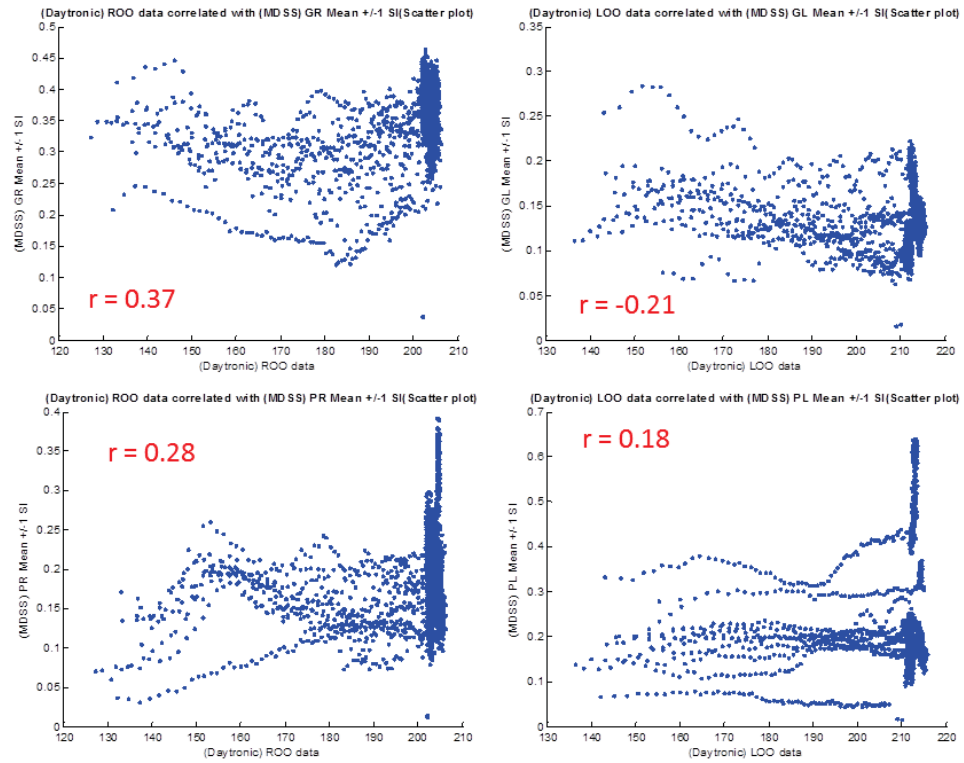


Figure 23: Correlation Between  $\pm 1$  Average Sideband (SI1) and Outlet Oil Temperatures.

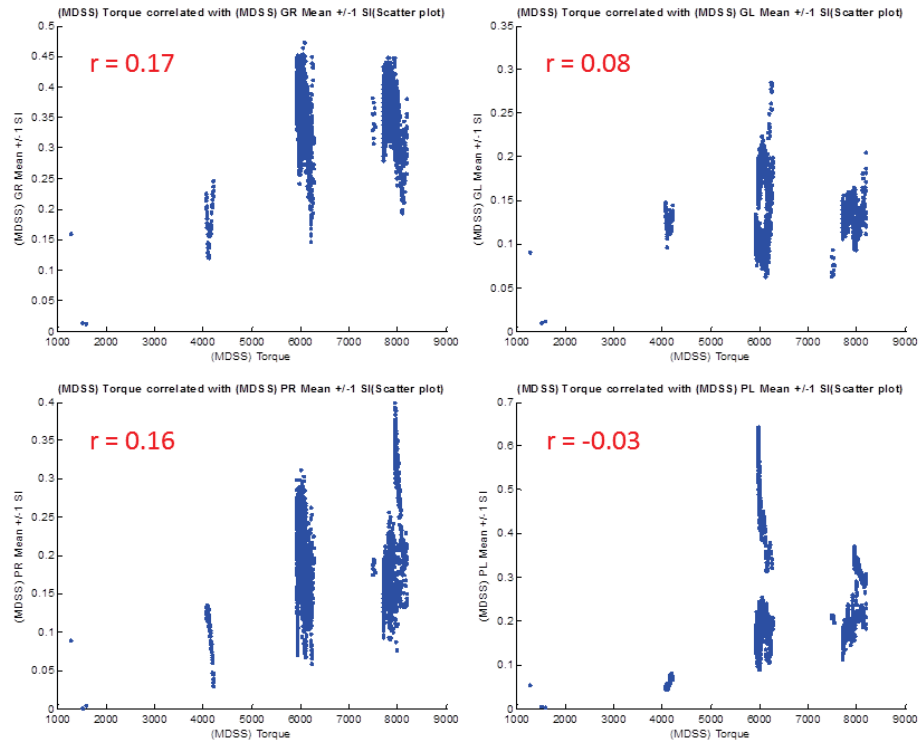


Figure 24. Correlation Between  $\pm 1$  Average Sideband (SI) and Torques.

Correlation analysis determined that some CIs were sensitive to operating conditions during test 1. However, the correlation data was not separated into specific failure modes and levels of damage. Sensitivity of a gear CI to environmental conditions may increase or decrease based on damage. Non-linear correlations may also exist between CIs, damage modes and operating conditions that will require further analysis with different methods. Further studies are required to investigate these effects. Additional analysis methods and capabilities are planned for the tool that enables grouping the data into comparable damage levels for analysis.

**Summary:** The objective of this work was to demonstrate the benefit of a software tool used to fuse the data generated from three data acquisitions systems and damage progression photos during spiral bevel gear damage progression tests in the NASA Glenn Spiral Bevel Gear Fatigue Test Rig. The response of gear CIs RMS, FM4 and average sideband indexes were compared to gear tooth damage progression, gearbox oil temperatures and applied torque. The tool enabled comparison of CI performance for different damage modes. CI data was also correlated with the operational conditions that the gear sets were exposed to during damage initiation and progression. Results found sensitivities of some CIs to damage modes, levels of damage and environmental conditions that must be taken into consideration when developing reliable gear health monitoring tools. Lessons learned during this preliminary investigation will be used to define additional analysis methods to be incorporated into the data fusion tool.



## References

- [1] Handschuh, R.F.: Thermal Behavior of Spiral Bevel Gears. NASA TM-106518, 1995.
- [2] Handschuh, R.F.: Testing of Face-Milled Spiral Bevel Gears at High-Speed and Load. NASA/TM—2001-210743, 2001.
- [3] Stewart, R.M. 1977. Some useful data analysis techniques for gearbox diagnostics. Machine Health Monitoring Group, Institute of Sound and Vibration Research, University of Southampton, Report MHM/R/10/77, July 1977.
- [4] Zakrajsek, J.J. 1989. An investigation of gear mesh failure prediction techniques. NASA TM-102340, AVSCOM TM 89-C-005.
- [5] Zakrajsek, J.J., Handschuh, R.F., and Decker, H.J. 1994. Application of fault detection techniques to spiral bevel gear fatigue data. Proceedings of the 48th Meeting of the Mechanical Failures Prevention Group. Office of Naval Research, Arlington, Virginia, pp. 93–104.
- [6] ANSI/AGMA 1010-E95. Appearance of Gear Teeth – Terminology of Wear and Failure.
- [7] Delgado, Irebert; Dempsey, Paula; Antolick, Lance and Wade, Dan: Continued Evaluation of Gear Condition Indicator Performance on Rotorcraft Fleet. Airworthiness, CBM, and HUMS Specialists' Meeting, February 11-13, 2013, Huntsville, Alabama.
- [8] Triola, Mario. Elementary Statistics. 6<sup>th</sup> edition. Addison-Wesley 1995.

**Acknowledgements:** The authors would like to thank the NASA Rotary Wing Project and Traci Stadtmueller and Paul Swindell of the FAA Technical Center for their assistance and support of this work.